



Predictive Controlled GSP Performance Improvement with an Integrated $\mathcal{H}_2/\mathcal{H}_\infty$

M. Rezaei Darestani^{*a}, A. A. Nikkhah^a, A. Khaki Sedigh^b

^aAerospace Department, Khaje Nasir Toosi University of Technology, Tehran, Iran

^bElectrical and Computer Department, Khaje Nasir Toosi University of Technology, Tehran, Iran

PAPER INFO

Paper history:

Received 25 December 2012

Revised in revised form 21 January 2013

Accepted 28 February 2013

Keywords:

3 Axis GSP

Predictive Control

$\mathcal{H}_2/\mathcal{H}_\infty$ Control

ABSTRACT

An integrated robust optimal control is presented to enhance the closed loop performance in the presence of disturbance and uncertainties, to ensure smooth tracking and elimination of high frequency disturbances especially in accurate systems with minimum power consumption. Simulation result of the proposed controller based on the combination of \mathcal{H}_2 and \mathcal{H}_∞ controllers is used to show the effectiveness of the proposed methodology. A 3 axis gyro-stabilized MIMO platform is considered and the results of the NLPID and a single \mathcal{H}_∞ controller are compared with the proposed $\mathcal{H}_\infty/\mathcal{H}_2$ controller.

doi: 10.5829/idosi.ije.2013.26.11b.04

NOMENCLATURE

D	Damping coefficient about output axis	T_{ni}	Net input torque of related axis
F_i	Servo-amplifier transfer function	U_C	Control input
H_y	Angular momentum of y axis gyro	U_f	Desired applied input
H_z	Angular momentum of z axis gyro	\bar{U}_0	Reference input
I_i	Total moment of inertia about output axis	U_{Pi}	Net applied output torque
J_i	Total moment of inertia about input axis	Y_p	Plant output
K	Spring constant about output axis	Greek Symbols	
$k(x, t)$	External structured disturbance nonlinear dynamic	σ_j	Absolute angular motion about output axis
$n(x, t)$	Unstructured external disturbance nonlinear dynamic		

1. INTRODUCTION

Robust control is a prescribed solution to the control of uncertain systems with various affecting disturbances. In recent years, the \mathcal{H}_2 and \mathcal{H}_∞ controller design techniques have been widely studied. Both have strong theoretical basis and are efficient algorithms for synthesizing optimal and robust controllers. Their combination, the mixed $\mathcal{H}_2/\mathcal{H}_\infty$ allows combining intuitive quadratic performance specifications of the \mathcal{H}_2

synthesis with robust stability requirements specifications expressed by the \mathcal{H}_∞ synthesis. Integration of these controllers leads to a superior closed loop performance in the presence of large uncertainties and disturbances [1-4].

Many difficulties in the integrated $\mathcal{H}_2/\mathcal{H}_\infty$ controller design exist, where the straightforward combination of the \mathcal{H}_2 with the \mathcal{H}_∞ methodologies results in a conservative solution, i.e. the algorithm may fail to find a controller even if one exists, or it may be possible to find another controller, which achieves better values for the two norms. In this paper, a mixed $\mathcal{H}_2/\mathcal{H}_\infty$ controller synthesis technique based on linear

*Corresponding Author Email: m.rezaei.d@gmail.com (M. Rezaei Darestani)

matrix inequalities (LMIs) to setup a dynamic output feedback controller with transformed input is proposed [5-7].

The proposed model in this paper is a 3 axis gyro-stabilized platform (GSP) that because of high sensitivity in stability, tracking and control performance requires a controller that considers all disturbances and uncertainties which exist in input, output or state of the system. Small errors in the control system in compensation of disturbances or uncertainties cause great integral error in long term for the whole system. These errors affect system setting and finally system design accuracy.

In this paper, a predictive controller combined with an integrated $\mathcal{H}_2/\mathcal{H}_\infty$ controller is proposed. This combination increases the performance and stability, compensates system disturbances in the presence of unmodeled system uncertainties and disturbances. There is a rich literature in this area of control system design. These studies include, robust output feedback controller for the mixed $\mathcal{H}_2/\mathcal{H}_\infty$ controller. Based on Genetic Algorithms (GAs) and linear matrix inequalities (LMIs), a hybrid algorithm for uncertain continuous-time linear systems is presented [1]. To overcome the need for multivariable method of designing controller of low order, direct reduced order mixed $\mathcal{H}_2/\mathcal{H}_\infty$ control for the short take-off and landing maneuver technology is demonstrated. [8]. Mixed $\mathcal{H}_2/\mathcal{H}_\infty$ control problem with reduced order controllers for time-varying systems in terms of the solvability of differential linear matrix inequalities and rank conditions is provided [9]. A mixed $\mathcal{H}_2/\mathcal{H}_\infty$ controller synthesis technique based on multi-objective optimization is used, where the optimized criteria are the \mathcal{H}_2 and \mathcal{H}_∞ norms. The method is compared with the existing methods for solving linear matrix inequalities (LMIs) and bilinear matrix inequalities (BMIs) [5]. For a class of singular problems, necessary and sufficient conditions are established, so that the posed simultaneous $\mathcal{H}_2/\mathcal{H}_\infty$ problem is solvable by state feedback controllers [6]. Fixed-structure discrete-time $\mathcal{H}_2/\mathcal{H}_\infty$ controller synthesis problem in the delta operator frame work is considered [7]. A new approach to mixed $\mathcal{H}_2/\mathcal{H}_\infty$ output feedback control synthesis is proposed. Use of non-smooth mathematical programming techniques to compute locally optimal $\mathcal{H}_2/\mathcal{H}_\infty$ controllers, which may have a pre-defined structure, is presented [2]. A robust hybrid motion/force controller for rigid robot manipulators is presented. The main contribution of this study is that the proposed hybrid control system is able to accomplish motion objectives in free directions and force objectives in constrained directions under parametric uncertainty both in robot dynamics and stiffness constraint constant [10]. LTI and qLPV $\mathcal{H}_2/\mathcal{H}_\infty$ controllers are compared. The Pareto limit is used to show the compromise that has to be done when

a mixed synthesis is achieved [3]. A stochastic \mathcal{H}_∞ and a mixed, stochastic, $\mathcal{H}_2/\mathcal{H}_\infty$ control problem for discrete-time systems are considered and solved. Conditions for existence of a solution are derived, based on the solvability of an equivalent mini-max problem [4]. A collection of methods for improving the speed of MPC, using online optimization is described. These custom methods, which exploit the particular structure of the MPC problem, can compute the control action on the order of 100 times faster than a method that uses a generic optimizer [11], and so on [12-16].

Here a special combination of robust optimal control to have a smooth tracking, a model predictive controller (MPC) and an integrated $\mathcal{H}_2/\mathcal{H}_\infty$ control to high frequency disturbance rejection with a transformed input vector of cost function in a 3 axis coupled GSP is proposed.

This paper is organized as follows. In section two, 3 axis GSP model is derived. In section three, robust and optimal control theory and their combination is extended. In section four, the simulation results of the robust optimal methodologies to control and stabilize the system are demonstrated and finally results of the proposed controller with nonlinear PID (NLPID) and single \mathcal{H}_∞ control are compared.

2. THREE AXIS GSP MODELING

With the use of mechanical gyros in a GSP structure, its model has been derived. The mathematical model of the mechanical gyro is based on the Euler equation of motion for a solid object where its center of mass is located on its center of rotation. Symbolic equation of motion is [17]:

$$M = \dot{H} + \omega \times H \quad (1)$$

The equation of motion of a single axis gyro with output axis θ_z and the input axis ϕ_y and the input-output axis moments ($T_n - U_p$) is as follows [17]:

$$T_n = J_y \cdot s^2 \cdot \phi_y + H \cdot s \cdot \theta_z \quad (2)$$

$$U_p = -H \cdot s \cdot \phi_y + (I \cdot s^2 + D \cdot s + K) \theta_z \quad (3)$$

that gives

$$\frac{\theta_z}{T_n} = \frac{H}{J_y \cdot (J_y \cdot s^2 \cdot \phi_y + H \cdot s \cdot \theta_z)} \quad (4)$$

and hence

$$s^2 \cdot \phi_y = \frac{T_n}{J_y} \quad (5)$$

$$(I \cdot s^2 + D \cdot s + K) \theta_z = H \cdot s \cdot \phi_y + U_p \quad (6)$$

Defining the system state, input and output as:

$$x = \begin{bmatrix} \phi_y \\ \dot{\phi}_y \\ \theta_z \\ \dot{\theta}_z \end{bmatrix}; \quad u = T_n; \quad y = \theta_z \quad (7)$$

gives:

$$\bar{x} = \begin{bmatrix} 0 & 1 & 0 & 0 \\ 0 & 0 & 0 & 0 \\ 0 & 0 & 0 & 1 \\ 0 & \frac{H}{I} & -\frac{K}{I} & -\frac{D}{I} \end{bmatrix} \bar{x} + \begin{bmatrix} 0 \\ \frac{1}{J} \\ 0 \\ 0 \end{bmatrix} u + \begin{bmatrix} 0 \\ 0 \\ 0 \\ \frac{U_p}{I} \end{bmatrix} \quad (8)$$

$$y = [0 \ 0 \ 1 \ 0]x \quad (9)$$

This type of gyro stabilized platform consists of 3 single axis stabilizers. In this arrangement sensitive axis of each gyro is in direction of each axis of the stabilized platform. In relation to the sensed deviation of input axis of gyro, moment has been exerted to the related axis of platform to stabilize that axis. The main problem of a 3 axis GSP is input and output axis coupling of each channel. In this stabilizer which its schematic view and gyros structure is shown in Figures 2 and 3, θ angle is related to the precision axis and ϕ is related to the rotation of input axis of stabilized platform gyros. As the structure of gyros on the platform is as Figure 3, the output angle of 3 axes is derived as the Equations (16) to (18). By considering axis coupling and use of single axis stabilized gyro, equation of motion of 3 axis gyro stabilized platform has been derived for each channel [17].

X channel:

$$s^2 \phi_x = \frac{T_{nx}}{J_y} \quad (10)$$

$$(I.s^2 + D.s + K)\theta_z = H_y.s.\phi_x + U_p \quad (11)$$

Y channel:

$$s^2 \phi_y = \frac{T_{ny}}{J_x} \quad (12)$$

$$(I.s^2 + D.s + K)\theta_x = H_z.s.\phi_y + U_p \quad (13)$$

Z channel:

$$s^2 \phi_z = \frac{T_{nz}}{J_y} \quad (14)$$

$$(I.s^2 + D.s + K)\theta_y = H.s.\phi_z + U_p \quad (15)$$

and considering the channels coupling of the stabilized platform, the channels outputs are:

$$\sigma_x = \theta_z + \phi_z \quad (16)$$

$$\sigma_y = \theta_x + \phi_x \quad (17)$$

$$\sigma_z = \theta_y + \phi_y \quad (18)$$

Also, the control signals and the disturbances of each channel are respectively, (i: x, y, z) [17]:

$$T_{ni} = T_{di} - T_{si} \quad (19)$$

$$T_{si} = F_i \cdot \sigma_i \quad (20)$$

As previously stated, the input moment causes precision of gyro to sense the θ angle. This sensor is installed in each channel of the stabilizer and the state space equation of a three axis platform is derived as follows:

$$\dot{\bar{X}} = A\bar{X} + B\bar{U} + \bar{U}_f \quad (21)$$

$$\bar{Y} = C\bar{X} \quad (22)$$

$$\bar{X} = \begin{bmatrix} \phi_x \\ \dot{\phi}_x \\ \theta_x \\ \dot{\theta}_x \\ \phi_y \\ \dot{\phi}_y \\ \theta_y \\ \dot{\theta}_y \\ \phi_z \\ \dot{\phi}_z \\ \theta_z \\ \dot{\theta}_z \end{bmatrix}; \quad \bar{U} = \begin{bmatrix} T_{nx} \\ T_{ny} \\ T_{nz} \end{bmatrix}; \quad \bar{Y} = \begin{bmatrix} \sigma_x \\ \sigma_y \\ \sigma_z \end{bmatrix} = \begin{bmatrix} \theta_z + \phi_z \\ \theta_x + \phi_x \\ \theta_y + \phi_y \end{bmatrix} \quad (23)$$

$$A = \begin{bmatrix} 0 & 1 & 0 & 0 & 0 & 0 & 0 & 0 & 0 & 0 & 0 & 0 \\ 0 & 0 & 0 & 0 & 0 & 0 & 0 & 0 & 0 & 0 & 0 & 0 \\ 0 & 0 & 0 & 1 & 0 & 0 & 0 & 0 & 0 & 0 & 0 & 0 \\ 0 & \frac{H}{I} & -\frac{K}{I} & -\frac{D}{I} & 0 & 0 & 0 & 0 & 0 & 0 & 0 & 0 \\ 0 & 0 & 0 & 0 & 0 & 1 & 0 & 0 & 0 & 0 & 0 & 0 \\ 0 & 0 & 0 & 0 & 0 & 0 & 0 & 0 & 0 & 0 & 0 & 0 \\ 0 & 0 & 0 & 0 & 0 & 0 & 0 & 1 & 0 & 0 & 0 & 0 \\ 0 & 0 & 0 & 0 & 0 & 0 & 0 & 0 & 0 & 0 & 0 & 0 \\ 0 & 0 & 0 & 0 & 0 & 0 & 0 & 0 & 0 & 0 & 0 & 0 \\ 0 & 0 & 0 & 0 & 0 & 0 & 0 & 0 & 0 & 0 & 0 & 1 \\ 0 & 0 & 0 & 0 & 0 & 0 & 0 & 0 & \frac{H}{I} & -\frac{K}{I} & -\frac{D}{I} & 0 \end{bmatrix}, \quad B = \begin{bmatrix} 0 \\ 0 \\ 0 \\ 0 \\ \frac{1}{J_x} & 0 & 0 \\ 0 & 0 & 0 \\ 0 & 0 & 0 \\ 0 & 0 & 0 \\ 0 & 0 & 0 \\ 0 & 0 & 0 \\ 0 & 0 & 0 \\ 0 & 0 & \frac{1}{J_x} \\ 0 & 0 & 0 \\ 0 & 0 & 0 \end{bmatrix} \quad (24)$$

$$U_f = \begin{bmatrix} 0 \\ 0 \\ 0 \\ \frac{U_{px}}{I_x} \\ 0 \\ 0 \\ 0 \\ 0 \\ 0 \\ 0 \\ \frac{U_{py}}{I_y} \\ 0 \\ 0 \\ 0 \\ 0 \\ \frac{U_{pz}}{I_z} \end{bmatrix} \quad (25)$$

$$C = \begin{bmatrix} 0 & 0 & 1 & 0 & 0 & 0 & 0 & 0 & 1 & 0 & 0 & 0 \\ 1 & 0 & 0 & 0 & 0 & 0 & 1 & 0 & 0 & 0 & 0 & 0 \\ 0 & 0 & 0 & 0 & 1 & 0 & 0 & 0 & 0 & 0 & 1 & 0 \end{bmatrix} \quad (26)$$

A controller to stabilize and ensure closed loop tracking of the MIMO linear time invariant model of the gyro-stabilized system must now be designed. Hence, output control of 3 axis stabilizer has been derived [17]:

$$U = U_0 - U_c \tag{27}$$

$$U_c = F.Y \tag{28}$$

$$\bar{F} = \begin{bmatrix} F_1 & 0 & 0 \\ 0 & F_2 & 0 \\ 0 & 0 & F_3 \end{bmatrix} \tag{29}$$

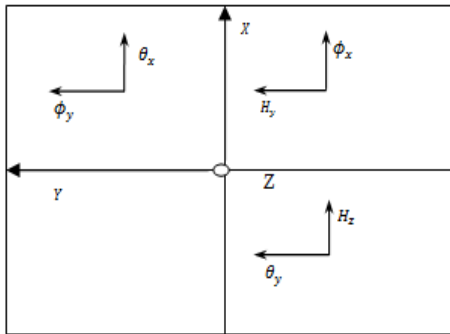


Figure 1. Gyro axis orientation on platform

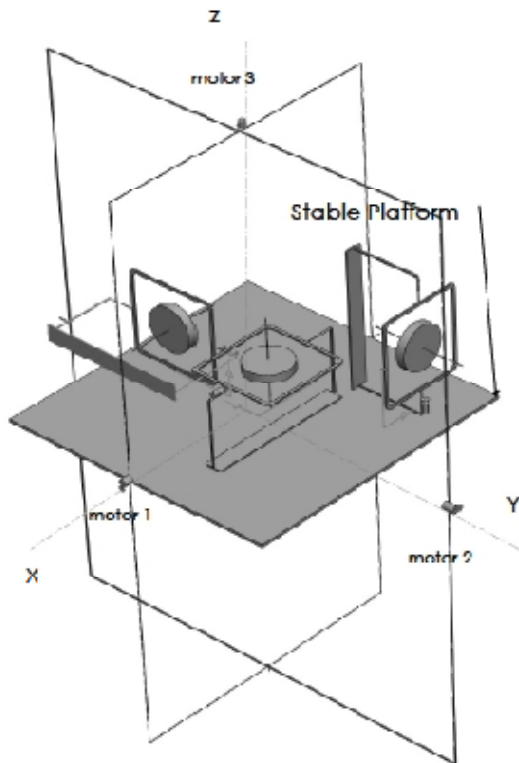


Figure 2. Schematic of 3 axis stabilized platform

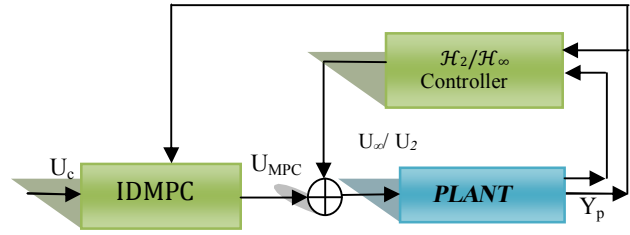


Figure 3. Proposed controller block diagram for the stabilized platform

3. GSP CONTROL IDEA

The proposed controller for the 3 axis GSP is an integrated controller that is a combination of $\mathcal{H}_2/\mathcal{H}_\infty$ in the inner loop and predictive control in the outer loop, which added integral/derivative of platform attitude to cost function parameters vector.

This combination uses benefits of predictive control to have a smooth tracking and reduction of low frequency time variant disturbances of a pre-defined trajectory, and a mixed $\mathcal{H}_2/\mathcal{H}_\infty$ controller to handle unknown uncertainties and compensating high frequency disturbances with minimum control force with the use of LMI theory.

Also, in predictive control with considering instantaneous receding horizon, system could overcome the sudden increase of input control signal and instability. Figure 4 shows block diagram of the proposed controller for the 3 axis GSP [18-20].

4. INTEGRAL/DERIVATIVE PREDICTIVE CONTROL

Predictive control is an optimal controller and provides high accuracy in tracking of the desired trajectory. The stabilized platform could reach to a high accuracy with proper selection of sensors and the selected structure of optimal controller. In the second step, with implementation of input commands, in the case of output disturbances, could reach to the desired accuracy of the system. In what follows, the cost function of the model predictive control (MPC), and the integral/derivative characteristics of the error are given. To design the predictive control state, space equation of the 3 axis GSP is used [14-16]:

$$\dot{X} = F(X,U) = AX(t) + BU(t) \tag{30}$$

$$Y = \begin{bmatrix} \sigma_x \\ \sigma_y \\ \sigma_z \end{bmatrix} = G(X) = C.X \tag{31}$$

To control the stabilized platform, it is assumed that the proposed platform is fixed on a set point or moves with an external command U_{pi} (usually $U_{pi} \approx 0$ in controller design) to a defined position. So a predefined trajectory for equation of motion of body without disturbances in ideal condition as the reference model is considered [14- 16]:

$$\dot{X}_r(t) = F(X_r, U_r) = AX_r(t) + BU_r(t) \tag{32}$$

$$Y_r = G(X_r) = C.X_r \tag{33}$$

where U_{ri} is the input reference moment and Y_{ri} is the output reference angle in each axis of the stable platform. This reference model has been used to define control input variations of the system in all conditions with or without disturbance. With these two defined models the error equation of the system is derived [12]:

$$\dot{X}_\zeta(t) = F(X_\zeta, U_\zeta) = AX_\zeta(t) + BU_\zeta(t) \tag{34}$$

$$Y_\zeta = G(X_\zeta) = C.X_\zeta \tag{35}$$

Now to reach to the desired control specifications, output error vector which consists of integral and derivative of the output error is:

$$\tilde{Y}_\zeta = H(\tilde{X}_n) = \begin{bmatrix} \tilde{\tau}_x \\ \dot{\tilde{\tau}}_x \\ \int \tilde{\tau}_x dt \\ \tilde{\tau}_y \\ \dot{\tilde{\tau}}_y \\ \int \tilde{\tau}_y dt \\ \tilde{\tau}_z \\ \dot{\tilde{\tau}}_z \\ \int \tilde{\tau}_z dt \end{bmatrix} = \begin{bmatrix} \sigma_x - \sigma_{xr} \\ \dot{\sigma}_x - \dot{\sigma}_{xr} \\ \int (\sigma_x - \sigma_{xr}) dt \\ \sigma_y - \sigma_{yr} \\ \dot{\sigma}_y - \dot{\sigma}_{yr} \\ \int (\sigma_y - \sigma_{yr}) dt \\ \sigma_z - \sigma_{zr} \\ \dot{\sigma}_z - \dot{\sigma}_{zr} \\ \int (\sigma_z - \sigma_{zr}) dt \end{bmatrix} \tag{36}$$

In the steady state, as $(t \rightarrow \infty)$, the output controlled error tend to reach to zero ($Y_\zeta \rightarrow 0$) and decreases the error of the whole system, as the system output tracks the reference path. The proposed controller is optimal with minimum energy consumption and could compensate output error changing. This condition with minimizing the following cost function in the proposed MPC has been assessed [14-16]:

$$J_z = [\tilde{Y}_\zeta - \tilde{Y}_{\zeta r}]^T Q [\tilde{Y}_\zeta - \tilde{Y}_{\zeta r}] + [\tilde{u}_\zeta - \tilde{u}_{\zeta r}]^T R [\tilde{u}_\zeta - \tilde{u}_{\zeta r}] + \Omega \{ \tilde{Y}_\zeta(k+N|k) - \tilde{Y}_{\zeta r}(k+N|k) \} \tag{37}$$

where R and Q are diagonal positive definite weighting matrices, and N is the control horizon. Also Ω is the cost of final states in the predictive system which is explained as [12, 16]:

$$\Omega \{ \tilde{Y}_\zeta(k+N|k) - \tilde{Y}_{\zeta r}(k+N|k) \} = [\tilde{Y}_\zeta(k+N|k) - \tilde{Y}_{\zeta r}(k+N|k)] Q_\zeta \cdot [\tilde{Y}_\zeta(k+N|k) - \tilde{Y}_{\zeta r}(k+N|k)] \tag{38}$$

and in the above equation Q_ζ is positive definite. Output prediction of the future step of discrete model of the system is [14, 15]:

$$\hat{\tilde{u}}_\zeta = \begin{bmatrix} \tilde{u}_{\zeta r}(k+1|k) - \tilde{u}_{\zeta r}(k|k) \\ \vdots \\ \tilde{u}_{\zeta r}(k+N+1|k) - \tilde{u}_{\zeta r}(k|k) \end{bmatrix} \tag{39}$$

$$\tilde{Y}_\zeta = \begin{bmatrix} \tilde{Y}_{\zeta r}(k+1|k) - \tilde{Y}_{\zeta r}(k|k) \\ \vdots \\ \tilde{Y}_{\zeta r}(k+N+1|k) - \tilde{Y}_{\zeta r}(k|k) \end{bmatrix} \tag{40}$$

and

$$\begin{bmatrix} Y_{\zeta k+1} \\ Y_{\zeta k+2} \\ \vdots \\ Y_{\zeta k+N} \end{bmatrix} = \begin{bmatrix} CA \\ CA^2 \\ \vdots \\ CA^N \end{bmatrix} \tilde{X}_\zeta + \begin{bmatrix} CB & 0 & \dots & 0 \\ CAB & CB & \dots & 0 \\ \vdots & \vdots & \dots & \vdots \\ CA^{N-1}B & \dots & CA^{N-L}B & 0 \end{bmatrix} \begin{bmatrix} \hat{\tilde{u}}_{\zeta k} \\ \hat{\tilde{u}}_{\zeta k+1} \\ \vdots \\ \hat{\tilde{u}}_{\zeta k+L} \end{bmatrix} \tag{41}$$

Minimizing the cost function of the predictive control without the constraints results in the following control law and this control signal has been used in the input control signal of the equation of motion of the system [12, 14-16]:

$$\hat{\tilde{u}}_\zeta = [H^T Q H + R]^{-1} \cdot [H^T Q (\hat{Y}_\zeta - S_\zeta X_\zeta(k)) + R \hat{\tilde{u}}_{\zeta r}] \tag{42}$$

which in every sampling time, k , only $\hat{\tilde{u}}_\zeta$ signal is required and finally the resulted control signal has been used in the GSP to reach an appropriate tracking.

5. MIXED $\mathcal{H}_2/\mathcal{H}_\infty$ CONTROLLER

In this section, an integration of a special type of robust optimal control, a mixed $\mathcal{H}_2/\mathcal{H}_\infty$ control is presented. This control system stabilizes the stable platform and must compensate all the unknown high frequency disturbances in the tracking loop of the predictive control with minimized control effort. This process must consider the optimal control signal boundary of the system especially in the presence of disturbances. We have [12, 21]:

$$\dot{X} = AX + B_\infty w_\infty + B_2 w_2 + B_u U \tag{43}$$

$$Z_\infty = C_\infty X + D_{\infty\infty} w_\infty + D_{\infty 2} w_2 + D_{\infty u} U \tag{44}$$

$$Z_2 = C_2 X + D_{2\infty} w_\infty + D_{22} w_2 + D_{2u} U \tag{45}$$

$$Y = C_y X + D_{y\infty} w_\infty + D_{y2} w_2 + D_{yu} U \quad (46)$$

where U is the input control vector, w_2 is the external structured disturbance vector, w_∞ is the unstructured external disturbance vector, and X , Y and Z are the state and output of the system. Let $D_{yu} = 0$ and to compute a finite value of the \mathcal{H}_2 norm $D_{22} = 0$ and also generally $D_{\infty 2} = D_{2\infty} = 0$, so [20-22]:

$$\dot{X} = AX + B_\infty w_\infty + B_2 w_2 + B_u U \quad (47)$$

$$Z_\infty = C_\infty X + D_{\infty\infty} w_\infty + D_{\infty u} U \quad (48)$$

$$Z_2 = C_2 X + D_{2u} U \quad (49)$$

$$Y = C_y X + D_{y\infty} w_\infty + D_{y2} w_2 \quad (50)$$

For high frequency disturbance attenuation, control of the first order derivative of platform attitude has been considered. Also, as in MPC, proportional, derivative and integral sequence of rate of change of platform attitude error has been considered in the error vector. The integral term accomplishes zero steady state error when steady disturbance error affects the system. For the case of output-feedback, a dynamic controller is assumed for each part of the \mathcal{H}_2 and \mathcal{H}_∞ controller. For the \mathcal{H}_2 controller:

$$\dot{\zeta}_2 = A_{k2} \zeta_2 + B_{k2} T_1 \tilde{y}_{\chi 1} \quad (51)$$

$$U_2 = C_{k2} \zeta_2 + D_{k2} T_1 \tilde{y}_{\chi 1} \quad (52)$$

and for the \mathcal{H}_∞ controller:

$$\dot{\zeta}_\infty = A_{k\infty} \zeta_\infty + B_{k\infty} T_2 \tilde{y}_{\chi 2} \quad (53)$$

$$U_\infty = C_{k\infty} \zeta_\infty + D_{k\infty} T_2 \tilde{y}_{\chi 2} \quad (54)$$

$$K_{Ci} : \begin{bmatrix} A_{ki} & B_{ki} \\ C_{ki} & D_{ki} \end{bmatrix} \quad (55)$$

In the first step to design this controller, to stabilize the system in the inner loop and compensation of high frequency disturbances, the output error considered for the above outputs are:

$$\tilde{y}_{\chi 1} = \begin{bmatrix} \tilde{\chi}_x \\ \dot{\tilde{\chi}}_x \\ \int \tilde{\chi}_x dt \\ \tilde{\chi}_y \\ \dot{\tilde{\chi}}_y \\ \int \tilde{\chi}_y dt \\ \tilde{\chi}_z \\ \dot{\tilde{\chi}}_z \\ \int \tilde{\chi}_z dt \end{bmatrix} = \begin{bmatrix} \sigma_x - \sigma_{xr} \\ \dot{\sigma}_x - \dot{\sigma}_{xr} \\ \int (\sigma_x - \sigma_{xr}) dt \\ \sigma_y - \sigma_{yr} \\ \dot{\sigma}_y - \dot{\sigma}_{yr} \\ \int (\sigma_y - \sigma_{yr}) dt \\ \sigma_z - \sigma_{zr} \\ \dot{\sigma}_z - \dot{\sigma}_{zr} \\ \int (\sigma_z - \sigma_{zr}) dt \end{bmatrix} = C_{11} \cdot \tilde{x}_{\chi 1} \quad (56)$$

$$C_{11} = \begin{bmatrix} 0 & 0 & 0 & 1 & 0 & 0 & 0 & 0 & 0 & 0 & 0 & 0 & 0 & 0 & 1 & 0 & 0 & 0 & 0 & 0 \\ 0 & 0 & 0 & 0 & 1 & 0 & 0 & 0 & 0 & 0 & 0 & 0 & 0 & 0 & 0 & 1 & 0 & 0 & 0 & 0 \\ 0 & 0 & 0 & 0 & 0 & 1 & 0 & 0 & 0 & 0 & 0 & 0 & 0 & 0 & 0 & 1 & 0 & 0 & 0 & 0 \\ 1 & 0 & 0 & 0 & 0 & 0 & 0 & 0 & 0 & 0 & 1 & 0 & 0 & 0 & 0 & 0 & 0 & 0 & 0 & 0 \\ 0 & 1 & 0 & 0 & 0 & 0 & 0 & 0 & 0 & 0 & 0 & 1 & 0 & 0 & 0 & 0 & 0 & 0 & 0 \\ 0 & 0 & 1 & 0 & 0 & 0 & 0 & 0 & 0 & 0 & 0 & 0 & 1 & 0 & 0 & 0 & 0 & 0 & 0 \\ 0 & 0 & 0 & 0 & 0 & 1 & 0 & 0 & 0 & 0 & 0 & 0 & 0 & 0 & 0 & 1 & 0 & 0 & 0 \\ 0 & 0 & 0 & 0 & 0 & 0 & 1 & 0 & 0 & 0 & 0 & 0 & 0 & 0 & 0 & 0 & 1 & 0 & 0 \\ 0 & 0 & 0 & 0 & 0 & 0 & 0 & 1 & 0 & 0 & 0 & 0 & 0 & 0 & 0 & 0 & 0 & 1 & 0 \\ 0 & 0 & 0 & 0 & 0 & 0 & 0 & 0 & 1 & 0 & 0 & 0 & 0 & 0 & 0 & 0 & 0 & 0 & 1 \end{bmatrix} \quad (57)$$

$$\tilde{x}_{\chi 1} = \begin{bmatrix} \dot{\phi}_x - \dot{\phi}_{xr} \\ \ddot{\phi}_x - \ddot{\phi}_{xr} \\ \int (\dot{\phi}_x - \dot{\phi}_{xr}) dt \\ \dot{\theta}_x - \dot{\theta}_{xr} \\ \ddot{\theta}_x - \ddot{\theta}_{xr} \\ \int (\dot{\theta}_x - \dot{\theta}_{xr}) dt \\ \dot{\phi}_y - \dot{\phi}_{yr} \\ \ddot{\phi}_y - \ddot{\phi}_{yr} \\ \int (\dot{\phi}_y - \dot{\phi}_{yr}) dt \\ \dot{\theta}_y - \dot{\theta}_{yr} \\ \ddot{\theta}_y - \ddot{\theta}_{yr} \\ \int (\dot{\theta}_y - \dot{\theta}_{yr}) dt \\ \dot{\phi}_z - \dot{\phi}_{zr} \\ \ddot{\phi}_z - \ddot{\phi}_{zr} \\ \int (\dot{\phi}_z - \dot{\phi}_{zr}) dt \\ \dot{\theta}_z - \dot{\theta}_{zr} \\ \ddot{\theta}_z - \ddot{\theta}_{zr} \\ \int (\dot{\theta}_z - \dot{\theta}_{zr}) dt \end{bmatrix} \quad (58)$$

$$\tilde{y}_{\chi 2} = \begin{bmatrix} \tilde{\chi}_x \\ \dot{\tilde{\chi}}_x \\ \int \tilde{\chi}_x dt \\ \tilde{\chi}_y \\ \dot{\tilde{\chi}}_y \\ \int \tilde{\chi}_y dt \\ \tilde{\chi}_z \\ \dot{\tilde{\chi}}_z \\ \int \tilde{\chi}_z dt \end{bmatrix} = \begin{bmatrix} \sigma_x - \sigma_{xr} \\ \dot{\sigma}_x - \dot{\sigma}_{xr} \\ \int (\sigma_x - \sigma_{xr}) dt \\ \sigma_y - \sigma_{yr} \\ \dot{\sigma}_y - \dot{\sigma}_{yr} \\ \int (\sigma_y - \sigma_{yr}) dt \\ \sigma_z - \sigma_{zr} \\ \dot{\sigma}_z - \dot{\sigma}_{zr} \\ \int (\sigma_z - \sigma_{zr}) dt \end{bmatrix} = C_{22} \cdot \tilde{x}_{\chi 2} \quad (59)$$

$$C_{22} = \begin{bmatrix} 0 & 0 & 0 & 1 & 0 & 0 & 0 & 0 & 0 & 0 & 0 & 0 & 0 & 0 & 1 & 0 & 0 & 0 & 0 & 0 \\ 0 & 0 & 0 & 0 & 1 & 0 & 0 & 0 & 0 & 0 & 0 & 0 & 0 & 0 & 0 & 1 & 0 & 0 & 0 & 0 \\ 0 & 0 & 0 & 0 & 0 & 1 & 0 & 0 & 0 & 0 & 0 & 0 & 0 & 0 & 0 & 0 & 1 & 0 & 0 & 0 \\ 1 & 0 & 0 & 0 & 0 & 0 & 0 & 0 & 0 & 0 & 1 & 0 & 0 & 0 & 0 & 0 & 0 & 0 & 0 & 0 \\ 0 & 1 & 0 & 0 & 0 & 0 & 0 & 0 & 0 & 0 & 0 & 1 & 0 & 0 & 0 & 0 & 0 & 0 & 0 \\ 0 & 0 & 1 & 0 & 0 & 0 & 0 & 0 & 0 & 0 & 0 & 0 & 1 & 0 & 0 & 0 & 0 & 0 & 0 \\ 0 & 0 & 0 & 0 & 0 & 1 & 0 & 0 & 0 & 0 & 0 & 0 & 0 & 0 & 0 & 1 & 0 & 0 & 0 \\ 0 & 0 & 0 & 0 & 0 & 0 & 1 & 0 & 0 & 0 & 0 & 0 & 0 & 0 & 0 & 0 & 1 & 0 & 0 \\ 0 & 0 & 0 & 0 & 0 & 0 & 0 & 1 & 0 & 0 & 0 & 0 & 0 & 0 & 0 & 0 & 0 & 1 & 0 \\ 0 & 0 & 0 & 0 & 0 & 0 & 0 & 0 & 1 & 0 & 0 & 0 & 0 & 0 & 0 & 0 & 0 & 0 & 1 \end{bmatrix} \quad (60)$$

$$\tilde{x}_{\chi 2} = \begin{bmatrix} \dot{\phi}_x - \dot{\phi}_{xr} \\ \ddot{\phi}_x - \ddot{\phi}_{xr} \\ \int (\dot{\phi}_x - \dot{\phi}_{xr}) dt \\ \dot{\theta}_x - \dot{\theta}_{xr} \\ \ddot{\theta}_x - \ddot{\theta}_{xr} \\ \int (\dot{\theta}_x - \dot{\theta}_{xr}) dt \\ \dot{\phi}_y - \dot{\phi}_{yr} \\ \ddot{\phi}_y - \ddot{\phi}_{yr} \\ \int (\dot{\phi}_y - \dot{\phi}_{yr}) dt \\ \dot{\theta}_y - \dot{\theta}_{yr} \\ \ddot{\theta}_y - \ddot{\theta}_{yr} \\ \int (\dot{\theta}_y - \dot{\theta}_{yr}) dt \\ \dot{\phi}_z - \dot{\phi}_{zr} \\ \ddot{\phi}_z - \ddot{\phi}_{zr} \\ \int (\dot{\phi}_z - \dot{\phi}_{zr}) dt \\ \dot{\theta}_z - \dot{\theta}_{zr} \\ \ddot{\theta}_z - \ddot{\theta}_{zr} \\ \int (\dot{\theta}_z - \dot{\theta}_{zr}) dt \end{bmatrix} \quad (61)$$

Therefore, the closed loop system is described as [20-22].

$$\begin{bmatrix} \dot{X}_{cl} \\ Z_{\infty} \\ Z_2 \end{bmatrix} = \begin{bmatrix} A_{cl} & | & B_{cl\infty} & B_{cl2} \\ - & - & - & - \\ C_{cl\infty} & | & D_{cl\infty} & D_{cl2} \\ C_{cl2} & | & E_{cl\infty} & 0 \end{bmatrix} \begin{bmatrix} X_{cl} \\ w_{\infty} \\ w_2 \end{bmatrix} \quad (62)$$

where

$$A_{cl} = \begin{bmatrix} A + B_u D_{kj} C_y & B_u C_{kj} \\ B_{kj} C_y & A_{kj} \end{bmatrix} \quad (63)$$

$$B_{cl\infty} = \begin{bmatrix} B_{\infty} + B_u D_k D_{y\infty} \\ B_k D_{y\infty} \end{bmatrix} \quad (64)$$

$$B_{cl2} = \begin{bmatrix} B_2 + B_u D_k D_{y2} \\ B_k D_{y2} \end{bmatrix} \quad (65)$$

$$C_{clj} = [C_j + D_{ju} D_{kj} C_y \quad D_{ju} C_{kj}] \quad (66)$$

$$D_{cl\infty} = [D_{\infty\infty} + D_{\infty u} D_{kj} D_{y\infty}] \quad (67)$$

$$D_{cl2} = [D_{\infty 2} + D_{\infty u} D_{kj} D_{y2}] \quad (68)$$

$$E_{cl\infty} = [D_{2u} D_{kj} D_{y\infty} + D_{2\infty}] \quad (69)$$

$$E_{cl2} = [0] \quad (70)$$

Using bounded real lemma and concept of the quadratic stability, the \mathcal{H}_{∞} constraint is equivalent to existence of a unique solution $X_{\infty} > 0$ that satisfies the matrix inequality:

$$\begin{pmatrix} A_{cl}^T X_{\infty} + X_{\infty} A_{cl} & X_{\infty} B_{cl\infty} & C_{cl\infty}^T \\ B_{cl\infty}^T X_{\infty} & -\gamma_{\infty}^2 I & D_{cl\infty}^T \\ C_{cl\infty} & D_{cl\infty} & -I \end{pmatrix} < 0 \quad (71)$$

and for the \mathcal{H}_2 performance measure, the \mathcal{H}_2 norm of T_{z2w} is derived as:

$$\|T_{z2w}\|_2^2 = Trace(C_{cl2} X_2 C_{cl2}^T) \quad (72)$$

where $X_2 > 0$ is the solution of the Lyapunov equation:

$$A_{cl} X_2 + X_2 A_{cl}^T + B_{cl} B_{cl}^T = 0 \quad (73)$$

that for the proposed uncertain system plant, $\|T_{z2w}\|_2^2 \leq Trace(C_{cl2} X_2^* C_{cl2}^T)$ for any $X_2^* > 0$ such that:

$$A_{cl} X_2^* + X_2^* A_{cl}^T + B_{cl} B_{cl}^T < 0 \quad (74)$$

It is important to notice that the Inequalities (71), (74) are LMIs are dependent to the fixed controller gains (K_{Ci}) and $\gamma_{\infty}, \gamma_2$.

Summarizing above relations derives integrated $\mathcal{H}_2/\mathcal{H}_{\infty}$ robust control problem matrix inequality as Equations (71) and (75)-(77):

$$\begin{bmatrix} A_{cl}^T X_2^* + X_2^* A_{cl} & X_2^* B_{cl2} \\ B_{cl2}^T X_2^* & -I \end{bmatrix} < 0 \quad (75)$$

$$\begin{bmatrix} X_2^* & C_{cl2}^T \\ C_{cl2} & Y_2 \end{bmatrix} > 0 \quad (76)$$

$$Trace(Y_2) < \gamma_2 \quad (77)$$

As stated in the recent studies [21], this problem is not convex in the variables (X_2, X_{∞}, K_C) , but it is convex for a fixed controller K_{Ci} . This performance criterion gives an upper bound of the optimal \mathcal{H}_2 performance subject to the \mathcal{H}_{∞} norm constraint. Here, it must be mentioned that our approach does not assume the hypothesis of common Lyapunov matrices, as it assume $X_2 = X_{\infty}$. Its advantage is conservatism reduction and better results generation. Also, the dynamic or static output feedback control case for plants subject to uncertainties is solvable [22].

This problem is solved by MATLAB LMI control toolbox by specified constraints. The combination of the \mathcal{H}_2 and \mathcal{H}_{∞} synthesis is done by combining (71), (75), (76) and (77) to a single LMI. A solution can be found again by setting γ_{∞} to a desired, achievable value and solving a $Trace(Y_2)$ minimization problem [20-22].

Problem definition in relation to the proposed controller setup in MATLAB and finding a suitable gain (K(s)) with LMI control toolbox is introduced as the following steps [22]:

Step 1: Plant definition as a MATLAB LTI system:

$$A = A; B = [B_{\infty} \quad B_2 \quad B_u]; C = [C_{\infty} \quad C_2 \quad C_u];$$

$$D = [D_{\infty\infty} \quad 0 \quad D_{\infty u}; \quad 0 \quad 0 \quad D_{2u}; \quad D_{y\infty} \quad 0 \quad D_{y2}],$$

$$P = \text{ltisys}(A, B, C, D)$$

that P is the system plant.

Step 2: Determine the integrated $\mathcal{H}_2/\mathcal{H}_{\infty}$ controller gain, $K(s)$:

$r = [3 \ 3 \ 3]$; that is a 1×3 vector listing the lengths of z_2, y and u

region-lmireg: Specifying and place the closed-loop poles in the lmi region.

obj= $[\gamma \ v \ \alpha \ \beta]$: vector specifying the $\mathcal{H}_2/\mathcal{H}_{\infty}$ objective.

$$[\text{gopt}, h2opt, K] = \text{hinfnmix}(P, r, \text{obj}, \text{region})$$

that optimal output-feedback controller gain, K , is defined with MATLAB functions [21, 22].

5.1. Stabilizing and Controlling Signal Integration Problem

The problem of integration of control signals is considered in this section. Two different control signals in the inner loop and outer loop are combined to stabilize and ensure tracking simultaneously. In the inner loop which has duty of stabilizing and compensating of high frequency disturbance of the system with minimized control effort, high frequency stabilizing signals are generated. These signals must be combined with the low frequency signals generated for tracking of the reference input. It must be mentioned that the high frequency signals are the corrector and compensator of the stabilizing tracker system and lie on the low frequency signals. These two signals do not have any conflict in control and stability process with each other.

6. GSP SIMULATION

System simulation is performed in two cases, with and without input stabilizing loop. A comparison study of the proposed controller and a NLPID control is performed. In the following simulation, results of the 3axis GSP are presented.

In the first section simulation, results are without the inner stabilizing loop which shows good tracking without platform stabilizing that system oscillates at the equilibrium point due to the interaction dynamics. These results have been generated with the use of MPC and NLPID controller in the outer loop or tracking loop of GSP which tunes the attitude of the platform in relation to the predefined reference. As shown in Figures 4, 5 and 6, MPC generated control command and tracking path has the value and frequency lower than the NLPID control, that the system oscillation in tracking mode is minimum.

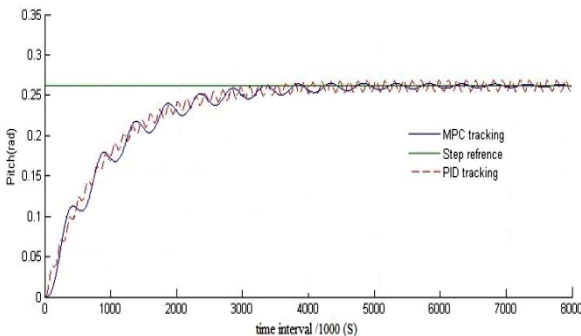


Figure 4. Comparison of NLPID control and MPC implementation without platform stabilizing

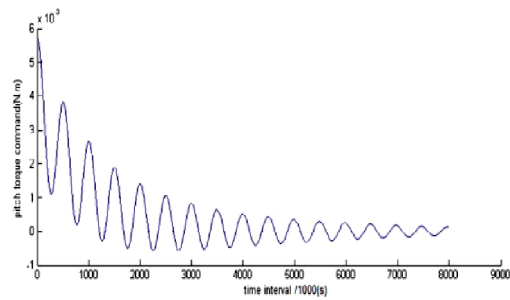
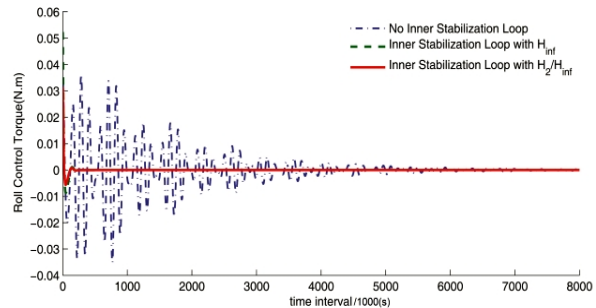
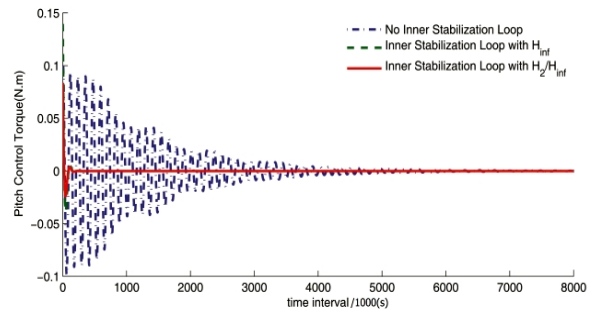


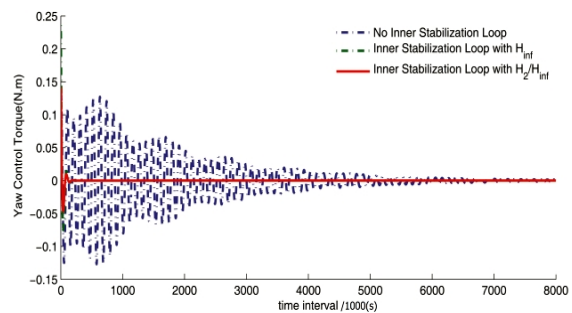
Figure 5. Pitch channel control command for MPC without platform stabilizing



(a) Roll



(b) Pitch



(c) Yaw

Figure 6. Channels control command comparison with and without GSP stabilizing

In the second step, the idea of system stabilizing with the use of an inner loop with application of error and its rate of changes for the proposed $\mathcal{H}_2/\mathcal{H}_\infty$ controller is implemented. In this section, as shown in Figure 6, the inner loop stabilized system with

minimum control effort with maximum disturbance rejection, and the outer loop achieves the tracking objective with the help of error changes. The simulations show that this idea is very appropriate for the system and platform in tracking process to have an accurate stable situation. The tracking and control effort comparison are shown in Figures 6 and 7. Main characteristics of the proposed controller show its advantages which make it more preferable than the other controllers as to be optimal, and compensate disturbances and uncertainty of the system. So, to show these characteristics in controlled system with NLPID and proposed controller, a known disturbance has been exerted to system and with equal tracking trajectory, generated control moment to each channel are compared. It is shown that the exerted control moment to each channel with the use of integrated controller is lower than the same moment which is generated by the NLPID and a single sub-optimal \mathcal{H}_∞ controller.

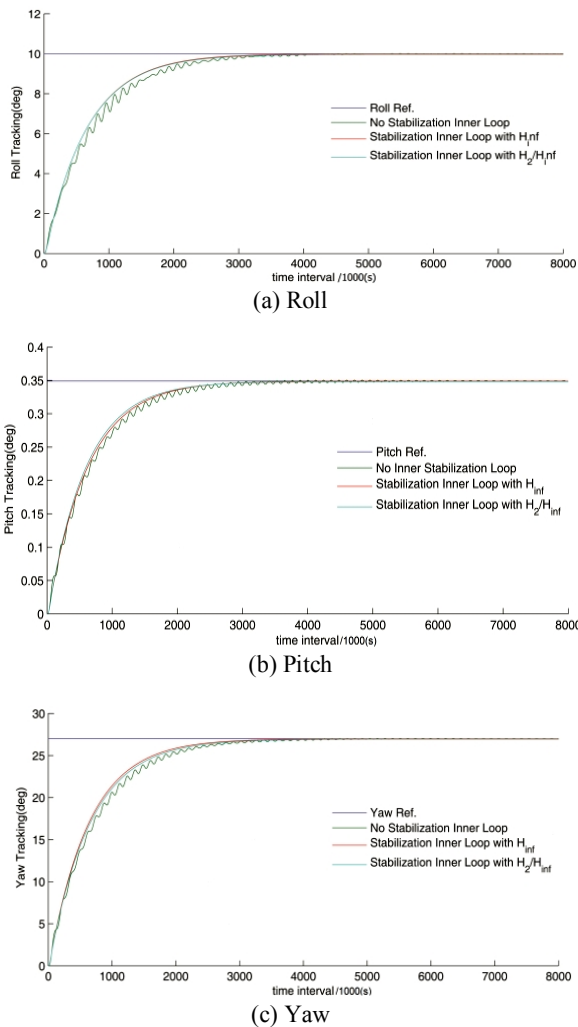


Figure 7. Implementation of integrated controller with platform stabilizing

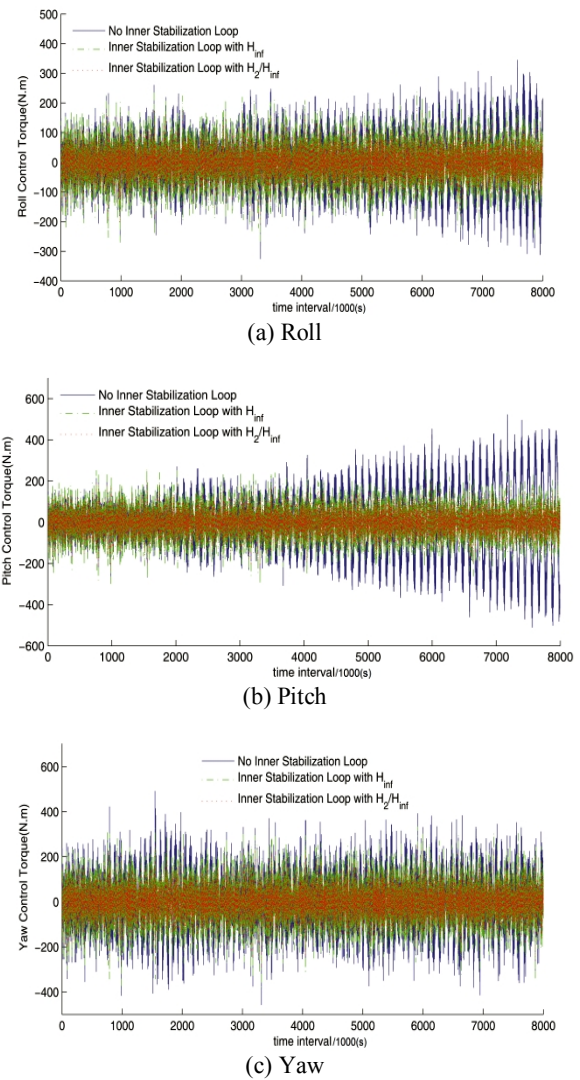


Figure 8. Comparison of channels control command for the implemented controllers with disturbance

7. CONCLUSION

The GSP has an oscillated line of sight, which complicates its control. The results show the effectiveness of the proposed controller in the presence of server disturbances to have a disturbance rejection and minimum power consumption at the same time.

8. REFERENCES

1. Pereira, G. J. and de Araujo, H. X., "Robust output feedback controller design via genetic algorithms and lmis: The mixed H_2/H_∞ problem", in American Control Conference, IEEE. Vol. 4, (2004), 3309-3314.
2. Apkarian, P., Noll, D. and Rondepierre, A., "Mixed H_2/H_∞ control via nonsmooth optimization", *SIAM Journal on Control and Optimization*, Vol. 47, No. 3, (2008), 1516-1546.

3. Poussot-Vassal, C., Sename, O., Dugard, L., Gaspar, P., Szabo, Z., and Bokor, J., "Multi-objective qLPV H_2/H_∞ control of a half vehicle", in Proceedings of the 10th Mini Conference on Vehicle System Dynamics, Identification and Anomalies, VSDIA. (2006).
4. Muradore, R. and Picci, G., "Mixed H_2/H_∞ control: The discrete-time case", *Systems & Control Letters*, Vol. 54, No. 1, (2005), 1-13.
5. Popov, A., "Less conservative mixed H_2/H_∞ controller design using multi-objective optimization", *Technical University of Hamburg*, (2005).
6. Rotea, M. A. and Khargonekar, P. P., " H_2 -optimal control with an H_∞ -constraint state feedback case", *Automatica*, Vol. 27, No. 2, (1991), 307-316.
7. Erwin, R. S. and Bernstein, D. S., "Fixed-structure discrete-time H_2 -optimal controller synthesis using the delta operator", in American Control Conference, IEEE. Vol. 5, (1997), 3185-3189.
8. C., W. and Jr., R., "Direct reduced order mixed h_2/h_∞ control for the short take-off and landing maneuver technology demonstrator (stol/mtd)", Air Force Institute of Technology. (1994)
9. Scherer, C., "Mixed H_2/H_∞ control", Mechanical Engineering Systems and Control Group Delft University of Technology.
10. Mut, V., Postigo, J., Carelli, R. and Kuchen, B., "Robust hybrid motion-force control algorithm for robot manipulators", *International Journal of Engineering*, Vol. 13, No. 4, (2000), 55-64.
11. Wang, Y. and Boyd, S., "Fast model predictive control using online optimization", *Control Systems Technology, IEEE Transactions on*, Vol. 18, No. 2, (2010), 267-278.
12. Raffo, G. V., Ortega, M. G. and Rubio, F. R., "An integral predictive/nonlinear H_∞ control structure for a quadrotor helicopter", *Automatica*, Vol. 46, No. 1, (2010), 29-39.
13. De Caigny, J., Camino, J. F., Oliveira, R. C., Peres, P. L. D. and Swevers, J., "Gain-scheduled \mathcal{H}_2 and \mathcal{H}_∞ control of discrete-time polytopic time-varying systems", *IET Control Theory & Applications*, Vol. 4, No. 3, (2010), 362-380.
14. Camacho, E. F. and Bordons, C., "Model predictive control", Springer London, Vol. 2, (2004).
15. Kuhne, F., Lages, W. F. and da Silva Jr, J. M. G., "Point stabilization of mobile robots with nonlinear model predictive control", in Mechatronics and Automation, International Conference, IEEE. Vol. 3, (2005), 1163-1168.
16. Giovanini, L. L., "Predictive feedback control", *ISA Transactions*, Vol. 42, No. 2, (2003), 207-226.
17. Mitsutomi, T., "Characteristics and stabilization of an inertial platform", *Aeronautical and Navigational Electronics, IRE Transactions on*, No. 2, (1958), 95-105.
18. Schaft, A. V. D. and Schaft, A., " L_2 -gain and passivity in nonlinear control", Springer-Verlag New York, Inc., (1999).
19. Geromel, J. C., Peres, P. and Souza, S., "Convex analysis of output feedback control problems: Robust stability and performance", *Automatic Control, IEEE Transactions on*, Vol. 41, No. 7, (1996), 997-1003.
20. Scherer, C., Gahinet, P. and Chilali, M., "Multiobjective output-feedback control via lmi optimization", *Automatic Control, IEEE Transactions on*, Vol. 42, No. 7, (1997), 896-911.
21. Ghany, A. M. A. and Alghmdy, A. G., Mixed H_2/H_∞ with pole-placement design of robust lmi-based output feedback controller for a.C turbo-generator power system connected to infinite bus, in 5th Saudi Technical Conference & Exhibition *STCEX*: Riyadh, Saudi Arabia, (2009)
22. Gahinet, P., Nemirovski, A., Laub, A. and Chilali, M., "MATLAB LMI control toolbox", *The MathWorks Inc*, (1995).

Predictive Controlled GSP Performance Improvement with an Integrated $\mathcal{H}_2/\mathcal{H}_\infty$ TECHNICAL NOTE

M. Rezaei Darestani^a, A. A. Nikkhah^a, A. Khaki Sedigh^b

^aAerospace Department, Khaje Nasir Toosi University of Technology, Tehran, Iran

^bElectrical and Computer Department, Khaje Nasir Toosi University of Technology, Tehran, Iran

PAPER INFO

چکیده

Paper history:

Received 25 December 2012

Recivede in revised form 21 January 2013

Accepted 28 February 2013

Keywords:

3 Axis GSP

Predictive Control

$\mathcal{H}_2/\mathcal{H}_\infty$ Control

به جهت بهبود کارایی سیستم حلقه بسته در حالت وجود اغتشاشات و نامعینی‌ها، برای اطمینان از دست‌یابی به ردگیری یکنواخت و حذف اغتشاشات فرکانس بالا مخصوصاً در سیستم‌های دقیق با حداقل توان مصرفی ترکیبی از کنترل بهینه مقاوم ارائه گردیده است. نتایج شبیه‌سازی کنترل‌کننده پیشنهادی بر اساس ترکیبی از کنترل‌کننده‌های \mathcal{H}_2 و \mathcal{H}_∞ برای نمایش تاثیر روش مفروض بیان گردیده است. در این مقاله یک نمونه پایدارکننده ژيروسکوپ ۳ محوره چند ورودی/چند خروجی در نظر گرفته شده و نتایج شبیه‌سازی کنترل‌کننده‌های NLPID و \mathcal{H}_∞ با کنترل‌کننده $\mathcal{H}_\infty/\mathcal{H}_2$ پیشنهادی مقایسه گردیده است.

doi: 10.5829/idosi.ije.2013.26.11b.04